

Straw Degradation Behaviors under Different Conditions of Relative Air Humidity and Ultraviolet-A Irradiation

Yunlong Li,^{a,b} Hongying Huang,^{a,*} Guofeng Wu,^a and Zhizhou Chang^a

In this study, straw was degraded continuously for 150 days under one of three levels of relative air humidity (RH) (90%, 60%, or 30%) to estimate the effect of humidity on straw biodegradation. Moreover, straw was treated with ultraviolet (UV)-A irradiation + 90% RH for 180 days to evaluate the interaction between photodegradation and biodegradation. The effects of 30% and 60% RH on straw degradation was inconspicuous. Straw mass losses at 90% RH and UV-A + 90% RH were 18.5% and 39.1%, respectively. BIOLOG analysis showed that filamentous fungi played a major role in straw biodegradation. Thermogravimetric analysis showed that treatment with UV-A + 90% RH tended to increase the maximum pyrolysis rate and decreased the initial pyrolysis temperature. Compared with 90% RH, infrared spectra analysis showed that functional groups of UV-A + 90% RH treatment, e.g., –CH, –C=O, and the benzene ring structure, clearly decreased. Straw-degrading bacteria were observed by scanning electron microscopy at the beginning and end of UV-A + 90% RH treatment. Results highlight the role of humidity in the degree of straw biodegradation by filamentous fungi. Straw degradation is accelerated by the combined action of photodegradation and biodegradation under high UV-A irradiation and high humidity.

Keywords: Relative air humidity; Ultraviolet-A irradiation; Photodegradation; Biodegradation; TGA; ATR-FTIR; BIOLOG; SEM

Contact information: a: Institute of Agricultural Resources and Environment, Jiangsu Academy of Agricultural Science, Nanjing, 210014, P.R. China; b: College of Life Sciences, Nanjing Normal University, Nanjing, 210023, P. R. China; *Corresponding author: huanghongyingvip@sina.com

INTRODUCTION

The degradation of crop residue has been shown to be closely associated with the global carbon cycling (Smith *et al.* 2010; Liu *et al.* 2014). In recent years, the relationships between environmental factors such as moisture, ultraviolet irradiation, atmospheric carbon dioxide, temperature, and degradation of crop residue has been given more and more attention (Schade *et al.* 1999; Austin and Vivanco 2006). In most models, built around the above-mentioned drivers, micro-biological degradation and photodegradation have been considered to be the most efficient pathways for the degradation of lignocellulosic materials (Zepp *et al.* 2007; Uselman *et al.* 2011).

Lignocellulosic materials are full of carbonaceous compounds, such as cellulose, hemicellulose, lignin, and dissolved organic matter (Smith *et al.* 2010; Liu *et al.* 2015). These carbon-containing compounds are utilized as carbon sources in the metabolic process of biomass-degrading microorganisms in the environment. With a change in the quantity, activity, and functional diversity of the microbial community, obvious mass losses in lignocellulosic materials have been observed during biodegradation. A wide

variety of enzyme systems are generated during microbial metabolism, which plays a crucial role in the degradation process (Wihan 2007; Buraimoh *et al.* 2015; Mohanram *et al.* 2015). Compared with the biodegradation of crop residue, which is mostly driven by straw-degrading microorganisms, the exact process of photodegradation has not been clearly expounded (Baker and Allison 2015). In general, lignin is considered to be resistant to environmental microorganisms during biodegradation, but it is susceptible to ultraviolet (UV) radiation with diverse wavelengths. Much early research suggests that many functional groups in lignin, *e.g.*, carboxide, phenylbenzene, aldehyde group, and conjugated double bonds are capable of absorbing ultraviolet radiation and reacting with active oxygen as the main promoter of photodegradation (Lanzalunga and Bietti 2000; Austin and Ballaré 2010; Rosu *et al.* 2010). In addition, a free radical mechanism of photo-induced oxidation of lignocellulosic materials was shown to involve a chain reaction in the liquid phase (Malešič *et al.* 2005). Early studies suggested that a variety of carbon-centred free radicals are formed with the extension of ultraviolet irradiation, to which the addition of oxygen forms peroxy radicals. Hydrogen was abstracted by peroxy radicals to form hydroperoxides. Exposed under conditions of increased ultraviolet radiation may result in homolytic degradation of hydroperoxides, yielding various active hydroxyl free radicals. Due to the high activity of hydroxyl free radicals, hydroxyl radicals react with carbonaceous compounds and abstract hydrogen atoms bonded to them (Bailey 1985; Kolar 1997; Malešič *et al.* 2005). Cellulose and hemicellulose are degraded by free radicals and active oxygen after the degradation of partial lignin (Gould 1982; King *et al.* 2012; Li *et al.* 2016).

Considerable research has shown that degradation is affected by experimental conditions (time, environment, and location) and material properties (type and composition) (Schade *et al.* 1999; Brandt *et al.* 2007; Day *et al.* 2007; Kirschbaum *et al.* 2011). In general, when crop residue is exposed to increased UV radiation under dry conditions, the photodegradation of biomass materials is primarily driven by UV irradiation through direct or indirect photolysis. In wet environments, biodegradation plays a more important role in the decomposition of lignocellulosic materials than photodegradation. Previous studies have shown that pretreatment with UV irradiation can promote microbial availability. However, the interaction between photodegradation and biodegradation of biomass materials under special environmental conditions with high UV irradiation and high moisture have not been fully elucidated.

A great deal of research has indicated degradation behaviors of biomass under soil burial or waterlogged conditions with UV supplementation (Fujii *et al.* 2014). Smith *et al.* (2010) found that the effect of UV irradiation on litter decomposition was dependent on the moisture availability. Liu *et al.* (2014) exposed waterlogged straw powder to UV irradiation and found that the effect of photodegradation on straw degradation was negative under wet conditions. However, few researchers have examined the degradation behavior of lignocellulosic material under different levels of relative air humidity (RH). Additionally, the action mechanism of biodegradation and photodegradation of biomass materials in moist conditions with UV supplementation has not been fully understood (Rozema *et al.* 1997; Lanzalunga and Bietti 2000).

The objective of this paper was as follows: (i) to examine biodegradation under different levels of relative air humidity; and (ii) to ascertain the interactive mechanism between photodegradation and biodegradation on the decomposition of lignocellulosic materials in moist conditions with UV-A supplementation.

EXPERIMENTAL

A straw decomposition experiment was set up using four different conditions: 30% RH (T₁), 60% RH (T₂), 90% RH (T₃), and UV-A + 90% RH (T₄).

Materials

Rice straw was obtained from Nanjing in Jiangsu Province, China. The straw was partially cut into 20-cm pieces (for T₄) and ground into 0.15-mm pieces for the relative air humidity treatments (T₁, T₂, and T₃); then, it was oven dried at 55 °C for 48 h.

Methods

Straw degradation under different levels of air relative humidity (T₁, T₂, and T₃)

In this experiment, different levels of relative air humidity were controlled by the saturated salt solution. At an ambient temperature of 30 °C, the solubilities of magnesium chloride (MgCl₂), sodium bromide (NaBr), and potassium nitrate (KNO₃) in water are 55.8 g, 98.4 g, and 45.8 g, respectively. The different levels of relative air humidity controlled by MgCl₂, NaBr, and KNO₃ in this study were 32.4% (± 0.56%), 56.0% (± 0.93%), and 92.3% (± 1.82%), respectively. Two liters of double-distilled water were added to a beaker and then heated to boiling. Excessive inorganic salt was added in batches and heated to dissolve. Then, the pellucid solution was poured into a vacuum shelf drier. The screened straw (20.0 ± 0.49 g) was added to the culture vessels (*D* = 12.0 cm). Then, the culture vessels were put into the vacuum shelf drier. All the containers were laid in an artificial climate box (MRC-300B, Ningbo Prandt Instrument Co., Ltd, China). The selected ambient temperature was 30 °C (± 0.81). The relative air humidity in each vacuum shelf drier was monitored regularly throughout the experiment. The samples were treated for 150 days, after which the culture vessels were taken out for subsequent analysis.

Straw degradation under UV-A + 90% RH (T₄)

The UV-A irradiation experiment was conducted in a UV generator (ZW-P, Yishi Co., Shanghai, China) for up to 180 d. The straw stems were tied to an iron plate (10 cm × 20 cm) vertically. Each plate was placed at a 45-degree angle to the ground in the UV generator. For this study, the radiation power was constant, at 1.5 KW/m², and the UV-A wavelength was 315 nm. Subsequently, the potassium nitrate saturated salt solution was poured into the UV generator. Ambient temperature (30 ± 2.3 °C) and relative air humidity (92.3% ± 1.4 RH) were continuously maintained and monitored by a hygrothermograph (JR593, Anymetre Instrument Co., Ltd., Guangzhou, China). The samples were removed and analyzed at each sampling date.

Analytical Methods

Mass loss

The straw mass under different conditions was recorded regularly. Samples were taken out and oven-dried at 55 °C to constant weight. The mass remaining (*R*) was calculated by Eq. 1,

$$R = W_t / W_0 \times 100\% \quad (1)$$

where *W*₀ is the weight of the straw before testing and *W*_{*t*} is the mass of treated straw at sampling date *t*.

Chemical composition

The concentrations of cellulose, hemicellulose, and lignin were determined by the Van-Soest method (Brandt *et al.* 2007). Dissolved organic carbon (DOC) and nitrogen (N) levels in the straw were quantified by the following method: 1 g of screened straw samples (0.15 mm) was poured into double-distilled water (50 mL) and then shaken for up to 5 h (180 rpm). Next, the tubes were centrifuged for 20 min at 4000 rpm. The supernatant was separated from a 0.50-mm film filter after standing for 20 min. The liquid was analyzed by an elemental analyzer (Multi N/C 3100 Analyzer, Analytik-Jena Group, Jena, Germany) (Song *et al.* 2011; Li *et al.* 2016). The contents of potassium (K) and phosphorus (P) were recorded by flame photometric analysis and spectrophotometry, respectively (Song *et al.* 2012).

The concentration remaining (R) in the chemical composition analysis was estimated using Eq. 2,

$$R = (W_t \times C_t) / (W_0 \times C_0) \times 100\% \quad (2)$$

where W_0 is the weight of straw before testing, C_0 is the initial concentration in the straw, and W_t and C_t are the weight and concentration of tested straw at sampling date t , respectively.

Thermogravimetric analysis

Thermogravimetric analysis (TGA; SII-7200, Hitachi Limited, Tokyo, Japan) was used to study the pyrolysis of the initial and final samples. Sieved samples (0.15 mm) were oven-dried and immediately used for the pyrolysis experiment.

Fourier transform infrared spectroscopy (FTIR)

The effect of T₃ and T₄ on the functional groups in straw was studied by FTIR (J200, Thermo Fisher Scientific, Waltham, USA). The samples were taken out at each sampling time and screened (0.15 mm), then oven-dried until constant weight.

BIOLOG microplate assays

The change in functional diversity of microbial communities in the straw was recorded by the BIOLOG plate technique. A total of 5 g of treated samples was collected from each sampling date and added into 45 mL of sterilized water immediately; then, the samples were shaken for 20 min (220 rpm). After being left to stand for 30 min, the supernatant (1 mL) was used for gradient dilution, and the final concentration of cell suspension was 10⁻³ g/mL (Garland and Mills 1991; Choi and Dobbs 1999).

Organism suspension (125 μL per well) was added to different types of microplates (ECO plates and FF plates) (P-96-450R-C, Genestar Limited, Shanghai, China), and ampicillin and streptomycin (50 μg/mL) were added to the FF plates to inhibit the growth of bacteria. The two types of plates were used for the study of the functional diversity of bacteria and filamentous fungi in the environment, respectively. The incubation temperature was 28 °C. The average well color development (AWCD) was read every 24 h at 578 nm and 490 nm. The values of AWCD were estimated using Eqs. 3 and 4, respectively:

$$AWCD_{ECO} = \sum (C_{it} - C_{0t}) / 31 \quad (3)$$

$$AWCD_{FF} = \sum (C_{it} - C_{0t}) / 95 \quad (4)$$

where C_{it} and C_{0t} are the absorbance of the sole carbon source and the control at time t . The Shannon-Wiener Diversity Index (H) was estimated using Eq. 5,

$$H = -\sum (P_i \times \ln P_i) \quad (5)$$

where $P_i = (C_i - R) / \sum (C_i - R)$, C_i is the absorbance of the sole carbon source well in the plate, and R is the absorbance of the control well.

Scanning electron microscope analysis

Scanning electron microscopy (SEM; EVO MA, Carl Zeiss Shanghai Co. Ltd., Shanghai, China) was used to study the surface morphological changes in the samples. Each specimen was gold plated for 60 s in a sputter-coater (ETD-2000, Beijing Elaborate Technology Development Ltd., Beijing, China), the coating thickness was about 10 nm.

Statistical analyses

Data were analyzed using the Software Statistical Package for Origin Pro (Version 9.0, OriginLab, Northampton, USA) and SPSS (Version 22.0, SPSS Inc., Chicago, IL).

RESULTS AND DISCUSSION

Mass Loss

The total straw mass losses for T_1 and T_2 were 3.7% and 5.7%, respectively (Fig. 1a). The straw mass for T_3 decreased more obviously, by 18.5%. Under the conditions of T_3 , mass loss was negligible at the beginning of the treatment (30 d). The maximum degradation rate occurred during days 30 through 60. Mass loss during this period increased by 17.1%, which accounted for 92.4% of the total. The effect of biodegradation on straw degradation was inconspicuous during the last 50 days. T_4 caused a drastic mass loss of 39.1% during the whole experiment, more than twice the mass loss of T_3 (Fig. 1b).

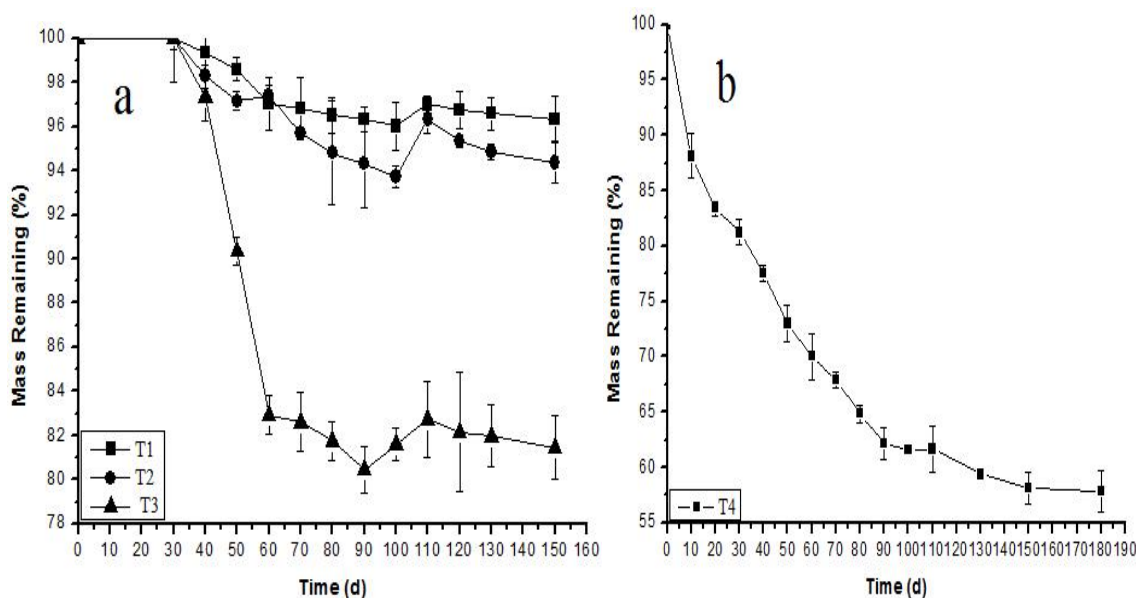


Fig. 1. Mass remaining of straw samples at each sampling date. (a) Mass remaining of 30% RH, 60% RH, and 90% RH. (b) Mass remaining of straw treated by UV + 90% RH

Under the condition of 90% RH, environmental microorganisms experienced a short adjustment period from days 0 to 30. Mass loss in this period was inconspicuous. During the subsequent 70 days, straw-degrading microorganisms entered an exponential growth phase. The maximum rate of degradation occurred in this 70-day period, which may be due to the abundant straw-degrading enzyme systems that were generated with the metabolism of straw-degrading microorganisms. Favorable conditions started to deteriorate after day 100. As a result, environmental microorganisms went into an apoptotic phase after day 100, and the straw decomposition rate gradually decreased until it was stable. Li *et al.* (2016) exposed dry rice straw to increased UV-A irradiation and found that long-term radiation decreased the straw mass by 5%. The mass loss of 39.1% provides strong evidence that degradation was accelerated both by photodegradation and biodegradation.

Elemental Characterization

Different treatments caused noticeable change to the elemental composition of straw. Compared with the control, organic carbon in T₃ and T₄ decreased by 9.8% and 13.9%, respectively. The concentration of nitrogen increased by 35.2% under the condition of UV-A + 90% RH, which was 1.7 times and 10.3 times the increase in straw N concentration at 90% RH and 60% RH, respectively. The value of straw C/N reduction for different conditions followed the order: T₄ > T₃ > T₂ > T₁. The C/N of T₄ and T₃ decreased by 36.2% and 25.2%, respectively. Straw phosphorus and potassium of T₄ decreased dramatically, by 64.3% and 81.0%, respectively.

Table 1. Initial and Final Concentration of Elements in Straw (mean ± SD, n = 3)

Treatment		C (%)	N (%)	P (%)	K (%)	C:N
Initial		48.9 ± 1.87a	0.88 ± 0.05c	0.14 ± 0.03a	1.26 ± 0.05a	55.6 ± 2.21a
150 d	T ₁	48.1 ± 0.36a	0.88 ± 0.03c	0.14 ± 0.03a	1.18 ± 0.03b	54.7 ± 2.95a
	T ₂	47.2 ± 1.05a	0.91 ± 0.04c	0.13 ± 0.02a	1.01 ± 0.02c	51.9 ± 2.00a
	T ₃	44.1 ± 1.41b	1.06 ± 0.06b	0.08 ± 0.03b	0.81 ± 0.03d	41.6 ± 1.15b
180 d	T ₄	42.2 ± 1.15b	1.19 ± 0.04a	0.05 ± 0.00b	0.24 ± 0.03e	35.5 ± 0.87c

Straw Chemical Composition Analysis

The concentration of straw hemicellulose showed the most obvious change under the condition of T₃, a decrease of 15.7% throughout the experiment. Cellulose and lignin decreased by 11.1% and 5.3% under the condition of 90% RH, respectively (Fig. 2a). The degradation rate of lignocellulose was negligible during the first 40 days of T₃. From day 40 onward, hemicellulose was first degraded quickly, and cellulose showed a relatively low degradation rate at the same time. During the subsequent 60 days, the mass loss of hemicellulose and cellulose accounted for 65.7% and 59.3% of the overall weight loss, respectively. The effect of humidity treatments on lignin degradation was unnoticeable throughout the experiment. Figure 2a shows that the content of DOC first decreased to the minimum and then increased as the experiment went on. During the first 60 days of T₃, DOC was reduced from 62.8 to 54.2 mg/g. The DOC content was 70.3 mg/g at the end of the experiment, a 12% increase.

DOC was the main carbon source of the lignocellulose-degrading microorganisms at the beginning of the experiment. After 60 days, lignocellulose was partially broken into lower-molecular weight organic matter with the exponential growth phase of

microbes, which counteracted the decline of DOC to a certain degree (Gallo *et al.* 2006). The contents of cellulose, hemicelluloses, and lignin drastically decreased, by 21.6%, 16.8%, and 44.9%, respectively, throughout the T₄ treatment (Fig. 2b). Lignin was degraded faster than cellulose and hemicellulose. The degradation rate of cellulose and hemicellulose increased rapidly after 30 days. It is worth noting that the degradation rate of cellulose exceeded the degradation rate of hemicellulose after 60 days. The DOC content decreased from 62.8 to 51.62 mg/g in the first 50 days. During the subsequent 60 days, the DOC concentration increased to 65.93 mg/g. DOC content decreased after day 110, and the final concentration was 49.41 mg/g.

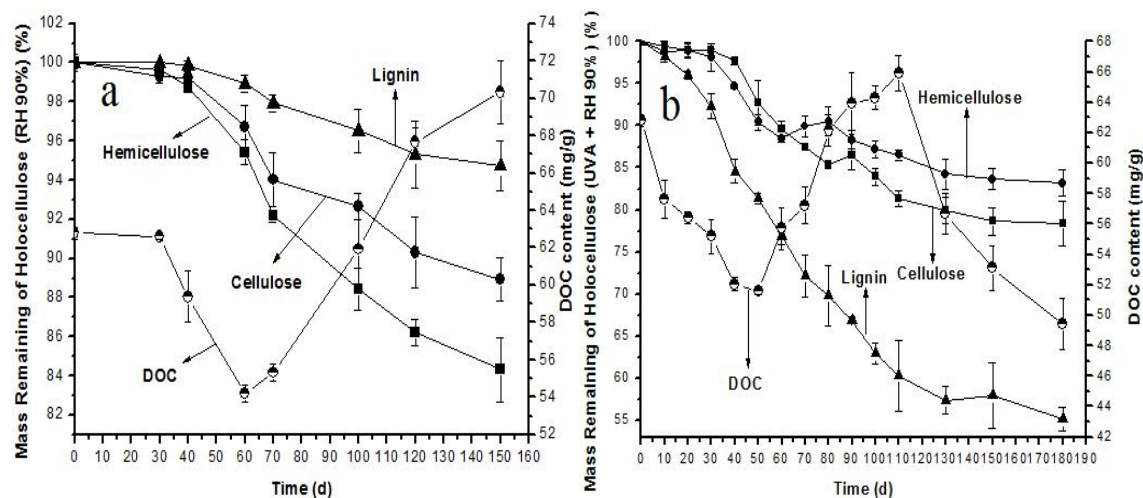


Fig. 2. Holocellulose remaining in straw samples: (a): 90% RH; (b): UV-A+ 90% RH. The error bars indicate standard deviation ($n = 3$).

As a result of utilization by straw-degrading microbes, the DOC concentration decreased drastically during the first 50 days of treatment. Most of the lignocellulose was degraded into a variety of small-molecular weight substances (Gallo *et al.* 2009; Grote *et al.* 2010). Lignin, as a polyphenolic compound, was degraded in a variety of ways with UV-A irradiation, such as the breaking of chemical bonds between lignin monomers and the rupture of benzene rings (Brandt *et al.* 2010; Smith *et al.* 2010). Cellulose and hemicellulose, surrounded by lignin, were then exposed to UV radiation and plentiful cellulolytic and hemicellulolytic enzymes as the lignin degradation progressed (Brink *et al.* 2014; Laothanachareon *et al.* 2015). As a result of the partial degradation of lignocellulose, the concentration of DOC increased from days 50 to 110. Compared with hemicellulose, a relatively high degradation rate of cellulose (in conditions T₄) after day 60 was consistent with the published values (Li *et al.* 2016). In contrast to the biodegradation of hemicelluloses for T₃, the degradation of lignin was the main reason for the mass loss of straw of (in conditions T₄), which indicated that photodegradation played a major role in the degradation of straw under a high-UV-A irradiation and a high-humidity environment. Although increased UV-A irradiation depressed the growth of microbes, the utilization of DOC at the beginning and end of the experiment implied that biodegradation still played an important role.

Thermogravimetric Analysis

The mass losses of the control, T₃, and T₄ samples during pyrolysis were 76.4%, 74.7%, and 70.8%, respectively (Fig. 3a). The temperature interval of the T₃ samples was

enlarged, which is contrary to the variation of the samples in conditions T₄. Treatment with 90% RH decreased the maximum pyrolysis rate and increased the maximum weight loss temperature from 350 to 380 °C. The maximum pyrolysis temperature of T₄ samples was 339 °C. The derivative thermogravimetry (DTG) curves showed that the maximum reaction rate of the control occurred at approximately 332 °C, and the temperatures of the maximum pyrolysis rate for T₃ and T₄ were 355 and 320 °C, respectively (Fig. 3b).

The pyrolysis process in straw started at approximately 200 °C, and the mass loss of straw before this stage was due to the loss of bound moisture (Zeng *et al.* 2011). The degradation of hemicellulose was the main reason for the mass loss of straw under the humidity treatments (Fig. 2a), which caused an increase in the relative concentration of lignin in straw. The enlarged temperature interval of T₃ was in relation to the relatively high concentration of lignin (Qu *et al.* 2015).

Contrary to the humidity treatment, cellulose, hemicelluloses, and lignin were all degraded drastically under the conditions of UV-A + 90% RH (Fig. 2b). The combined action of photodegradation and biodegradation caused not only the further degradation of straw but also an increase in mass loss and strengthening of the pyrolysis reaction (Fig. 3a). This is the main reason why the maximum reaction rate and the lowest energy consumption occurred in the pyrolysis of T₄.

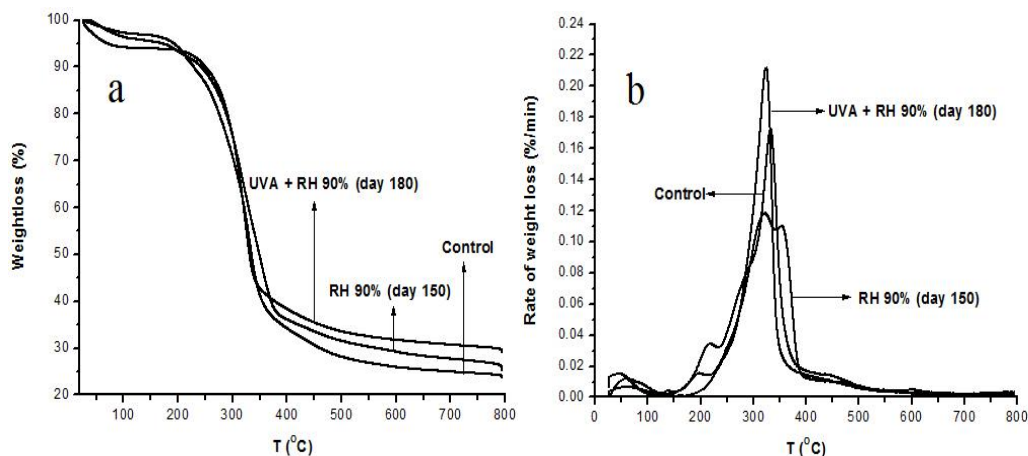


Fig. 3. Thermogravimetric analysis of control, 90% RH, and UV-A + 90% RH. (a) Mass losses of straw samples in the pyrolysis. (b) Derivative thermogravimetry curves of samples during the pyrolysis. Nitrogen atmosphere (flow rate: 20 mL/min). Temperature rate was 25 °C/min.

Fourier Transform Infrared Analysis

Figure 4 shows the infrared spectroscopy analysis of T₃ and T₄. The weaker peaks of T₃ at 2900 and 1740 cm⁻¹ were caused by the biodegradation of cellulose and hemicellulose, respectively (Fig. 4a). Compared with the control, the peaks near 1240 and 1030 cm⁻¹ showed a small reduction. This indicates that lignin in the straw was degraded by the microorganisms under the conditions of 90% RH.

The strong absorption peaks of T₄ samples at approximately 3350 and 2900 cm⁻¹ were caused by the stretching vibration of hydroxyl group (-OH) and aliphatic hydrocarbons (C-H), respectively (Fig. 4b). Compared with the control, absorption value in the two bands of T₄ showed obvious changes. The peak symmetry was almost the same, but the transmittance decreased, which belonged to decline of the characteristic absorption of the hydroxyl group and aliphatic hydrocarbons, respectively. The peak at 1740 cm⁻¹ was dominated by the carbonyl group (C=O). The decline of the peak at this

band was caused by the degradation of hemicellulose. The peaks at 1600 and 1580 cm^{-1} decreased drastically compared with those in the control, which were due to the benzene skeleton vibration in lignin (Pandey and Pitman 2003) and resulted in the rupture of the benzene rings. Peaks near 1382 cm^{-1} were caused by the stretching vibration of C-H in cellulose and hemicellulose (Müller *et al.* 2003). The weaker peak at this wave band indicated the degradation of cellulose and hemicellulose under the condition of UV-A + 90% RH. Peaks at 1317 and 1248 cm^{-1} were caused by the vibration of lignin monomers and ether linkages (Pandey and Pitman 2003; Huang *et al.* 2012). The peak at 1030 cm^{-1} was due to the C-H aromatic in-plane vibration. Weaker peaks at these bands further proved that lignin was degraded strongly by the elevated UV-A irradiation. Photodegradation played the major role in the degradation of lignocellulosic materials under the condition of UV-A + 90% RH.

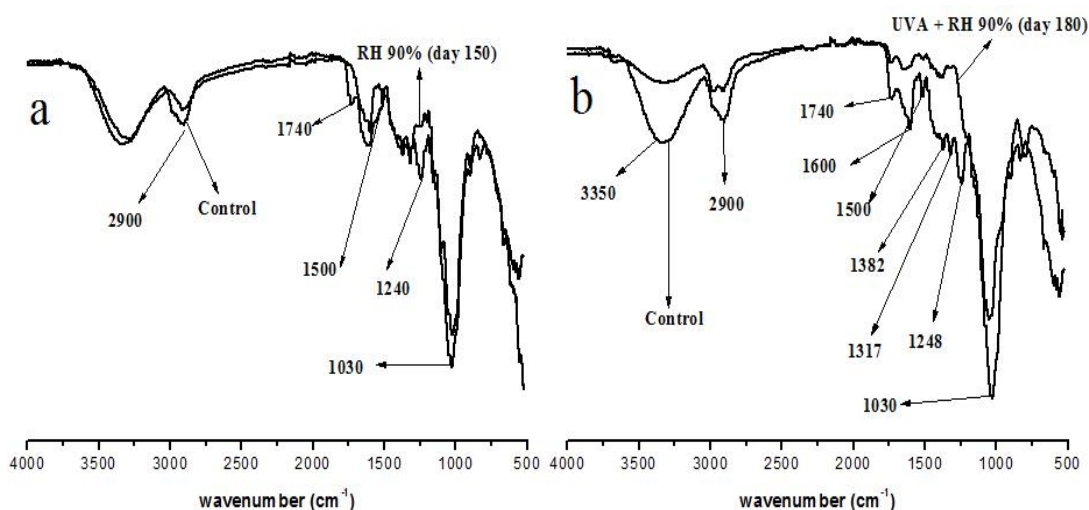


Fig. 4. Infrared spectroscopy analysis of initial and final samples under different conditions: (a) 90% RH. (b) UV-A + 90% RH

BIOLOG Microplates Assay

Average well color development (AWCD) reflects the ability of straw-degrading microorganisms to utilize the sole carbon source. It is important to reveal the change in microflora in a specific environment. Higher values of AWCD represent higher activity of environmental microbial communities (Hackett and Griffiths 1997; Fang *et al.* 2001).

With extended cultivation time, the values of AWCD showed an increasing trend (Fig. 5). During the first 24 h of cultivation, all the AWCD values of the various treatments were between 0.001 and 0.01, and the values increased rapidly after 24 h. Figure 5a shows the AWCD at different incubation times for T₃.

The AWCD values at days 0, 40, and 60 gradually increased at the end of incubation time and reached the maximum (0.095) at day 60. Microbial metabolic activity gradually decreased after day 60. The minimum value of AWCD was 0.05, which appeared at the end of the experiment.

Figure 5b shows the change in AWCD for T₂. Compared with T₃, the value of AWCD remained a lower level during the entire incubation. Microbial metabolic activity increased first and then decreased with treatment time. The maximum AWCD was 0.061, which appeared on day 100. The effect of T₁ on the microbial metabolic activity was not

obvious (Fig. 5c). The maximum and minimum values of AWCD were 0.024 and 0.009, respectively.

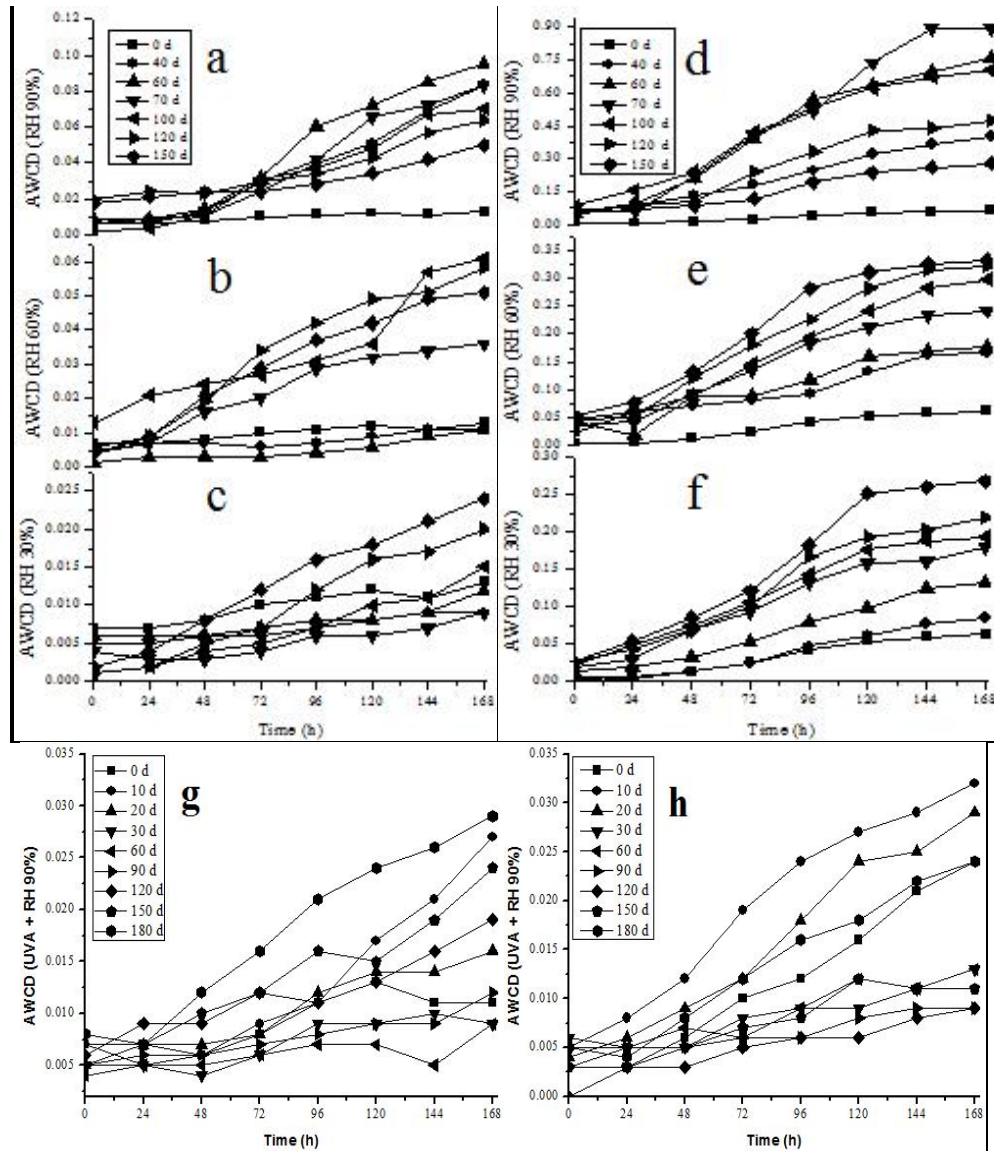


Fig. 5. Change in AWCD with duration of incubation in two BIOLOG plates: (a) 90% RH, (b) 60% RH, (c) 30% RH, and (g) UV-A + 90% RH for ECO plate; (d) 90% RH, (e) 60% RH, (f) 30% RH, and (h) (UV-A + 90% RH) for FF plate during an incubation time of 168 h

Figures 5d, 5e, and 5f show the change in AWCD for the FF plate. The values of AWCD formed typical S-shaped curves during the entire incubation time. The maximum value of AWCD was 0.893 in Fig. 5d, which appeared on the 70th day. It was approximately 2.7 times and 3.3 times the maximum values of AWCD of 60% RH and 30% RH, respectively, which both appeared on the 150th day (Fig. 5 e/f).

Figures 5g and 5h show the variation of AWCD in ECO plate and FF plate of T₄, respectively. The metabolic activity of environmental microorganisms increased during the first 10 days of T₄. The value of AWCD increased from 0.011 to 0.027 (Fig. 5g). The AWCD values of T₄ decreased to the minimum of 0.012 at approximately 90 days. The AWCD increased during the last 90 days, reaching a maximum of 0.029 at the end of the

experiment. The values of AWCD in the FF plate increased in the first 20 days and then decreased during the subsequent 100 days. The AWCD increased slightly after day 120 (Fig. 5h).

The values of AWCD in 90% RH was distinguishable from those for 30% RH and 60% RH. Results showed that higher humidity facilitated further biodegradation of lignocellulosic materials. It is worth reminding that the maximum value of AWCD appeared at approximately 70 days in both plates. This result is in line with previous results: the majority of mass loss occurred by approximately day 70 (Fig. 1). Moreover, compared with the data showed in ECO plates, values of AWCD in FF plates changed more obviously, from 0.27 (T₁) to 0.89 (T₃). These data indicated that the biodegradation of straw under different relative air humidity conditions was mostly accelerated by filamentous fungi. These results are consistent with previous studies (Martins *et al.* 2013; Yanto and Tachibana 2014).

With extended irradiation time, the increased UV-A radiation showed a noticeable inhibition against the environmental microorganisms. This is the reason why the values of AWCD decreased after day 20 in both plates. The small increase in AWCD at a late stage in the experiment was in line with previous results that suggest that biodegradation in a wet environment is facilitated by prolonged irradiation (Henry *et al.* 2008; Liu *et al.* 2015). The results further indicated that straw degradation under the conditions of UV-A + 90% RH was accelerated by the combined action of photodegradation and biodegradation. These results are in line with those in Figs. 2 and 3.

Microbial Functional Diversity Analysis

The Shannon-Wiener Diversity Index (H) is an important parameter reflecting the functional diversity of environmental microorganisms (Fierer and Jackson 2006). In the ECO plate, the variation range of H under the conditions of T₃ was 5.2 times and 8.7 times the range of T₂ and T₁, respectively (Table 2a). In the FF plate, the maximum H of T₃ was 1.7 times and 1.1 times the values of the initial and the end of experiment, respectively (Table 2b), and the variation range of H was 2.3 times and 2.7 times the range of T₂ and T₁, respectively. All the maximum values, in both plates, appeared on the 70th day. The variation in H showed a similar tendency as that of AWCD (Fig. 5).

Previous research showed that microbial activities are suppressed by increased UV irradiation (Santos *et al.* 2013; Yang and King 2014), and photodegradation has been regarded as the key driver of straw degradation in drought conditions (Brandt *et al.* 2007; Smith *et al.* 2010). However, the effect of lignocellulose-degrading microbes and the variation of microflora have constantly been underestimated at different stages of degradation under the condition of increased UV irradiation with high humidity.

Table 2c shows the functional diversity of microbial communities at different sampling dates for T₄. The functional diversity of environmental microorganisms increased at the beginning of the experiment, which caused a noticeable decrease in DOC (Fig. 2b). A small increase in the functional diversity of microbial communities was observed after day 90 in ECO.

The increased metabolic activity caused an apparent decrease in DOC, which was primarily generated during the degradation of macromolecular substances (Fig. 2b). These results implied that biodegradation played an important role at the beginning and end of the experiment in the conditions of UV-A irradiation with high humidity. In other words, the combined function of photodegradation and biodegradation facilitated the degradation of lignocellulosic materials under these conditions.

Table 2a. Shannon-Wiener Diversity Index of Environmental Microorganisms under Different Levels of Humidity (ECO plate) (n = 3)

Time (d)	RH (%)		
	30	60	90
0	2.06 ± 0.163	2.12 ± 0.211	2.01 ± 0.162
40	2.01 ± 0.032	2.03 ± 0.061	2.73 ± 0.215
60	1.93 ± 0.061	2.27 ± 0.012	4.21 ± 0.215
70	2.13 ± 0.113	2.29 ± 0.235	4.45 ± 0.436
100	2.16 ± 0.054	2.33 ± 0.136	3.74 ± 0.039
120	2.17 ± 0.281	2.41 ± 0.312	3.54 ± 0.066
150	2.21 ± 0.146	2.58 ± 0.194	3.01 ± 0.170

Table 2b. Shannon-Wiener Diversity Index of Environmental Microorganisms under Different Levels of Humidity (FF plate) (n = 3)

Time (d)	RH (%)		
	30	60	90
0	2.71 ± 0.099	2.66 ± 0.109	2.88 ± 0.332
40	2.56 ± 0.098	2.84 ± 0.216	3.69 ± 0.061
60	2.89 ± 0.046	3.02 ± 0.032	4.50 ± 0.105
70	3.00 ± 0.209	3.21 ± 0.077	4.82 ± 0.042
100	3.21 ± 0.016	3.31 ± 0.088	4.68 ± 0.112
120	3.33 ± 0.164	3.40 ± 0.081	4.72 ± 0.044
150	3.41 ± 0.074	3.52 ± 0.141	4.32 ± 0.229

Table 2c. Shannon-Wiener Diversity Index of Environmental Microorganisms under the Condition of UV-A + RH 90% (ECO and FF plate) (n = 3)

Time (d)	ECO plate	FF plate
0	2.07 ± 0.369	2.58 ± 0.248
10	2.41 ± 0.213	2.81 ± 0.381
20	2.32 ± 0.169	2.69 ± 0.266
30	1.81 ± 0.241	2.60 ± 0.311
60	1.17 ± 0.226	1.32 ± 0.162
90	1.21 ± 0.241	0.87 ± 0.211
120	1.46 ± 0.106	0.92 ± 0.301
150	1.59 ± 0.253	0.81 ± 0.209
180	1.72 ± 0.189	0.92 ± 0.162

Scanning Electron Microscopy

Compared with the control, many more straw-degrading microorganisms were observed on the 70th day for T₃ (Fig. 6a and Fig. 6b). The fiber structure was further disintegrated at the end of the treatment with 90% RH (Fig. 6c). However, few environmental microorganisms were observed at the end of 180-day experiment. Results further demonstrated that straw degradation was accelerated by biodegradation under 90% RH. Different from lignocellulose fracture by biodegradation, the effect of T₄ on the straw caused the shedding of flakes from the straw. Figure 6d shows the 10th day straw sample surface under the condition of UV-A + 90% RH. Compared with the acceleration of filamentous fungi on straw degradation, lignocellulosic straw-degrading bacteria played an important role during the first 10 to 20 days. Figure 6e shows the sample surface at the 90th day of T₄. Environmental microorganisms were inhibited with the extension UV-A irradiation. However, few straw-degrading bacteria were observed at the

end of the experiment (Fig. 6f). It should be specially mentioned that UV-resistant microorganisms were observed on the irradiated surface. Previous research showed that continuous exposure with increased UV irradiation under dry conditions could accelerate the subsequent biodegradation (Henry *et al.* 2008; Lin *et al.* 2015). It is still unknown whether biodegradation and photodegradation coexist under the conditions of increased UV with high humidity. Apparent straw-degrading microorganisms at the beginning and end of the experiment further proved that straw degradation under the condition of high UV irradiation with high humidity was accelerated by the combined action of photodegradation and biodegradation.

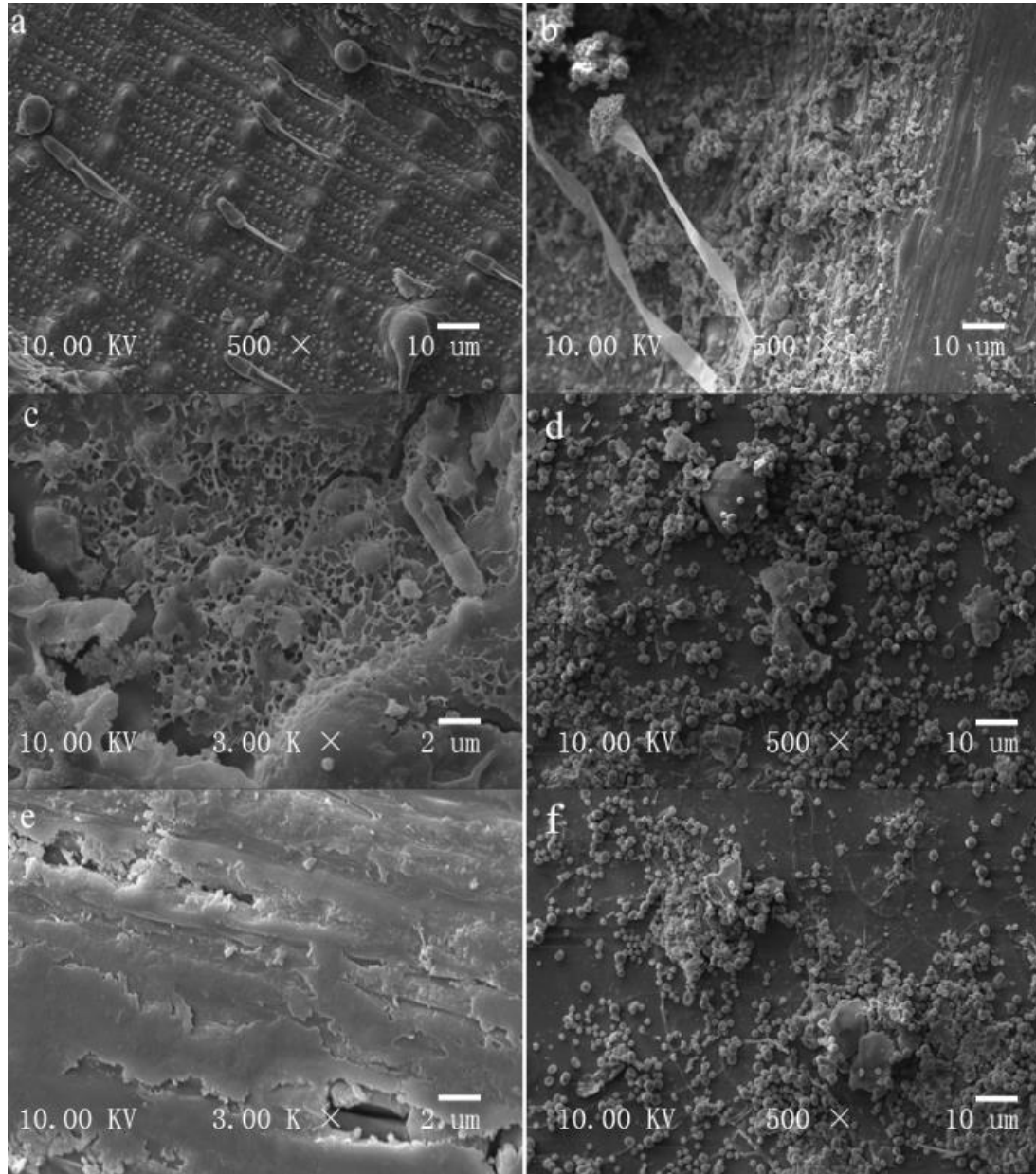


Fig. 6. SEM analysis of straw samples under the condition of 90% RH and UV-A + 90% RH. (a) Control. (b) sample surface of T₃ (70 d). (c) Disintegrated fiber structure of T₃ at day 150. (d) Sample surface of T₄ at day 10. (e) Fiber structure of T₄ at day 90. (f) Straw-degrading microbes on the sample surface of T₄ (180 d).

CONCLUSIONS

1. Straw mass losses with 30% RH and 60% RH were 3.7% and 5.7%, respectively. Compared with the two lower levels of humidity, 90% RH caused a larger decrease of straw mass, by 18.5%. Under the condition of 90% RH, the functional diversity of microbial communities increased first and then decreased and the maximum degradation rate occurred from days 60 through 70. The straw degradation was accelerated by filamentous fungi under the high-humidity conditions, which played a major role in the biodegradation.
2. Hemicellulose was degraded at a relatively high level during the whole biodegradation process, which led to an increase in the relative content of lignin at the end of the experiment. In the pyrolysis process, the lower maximum pyrolysis rate and the enlarged temperature interval occurred because of the relatively higher lignin content in the straw.
3. The straw mass decreased by 39.1% under the conditions of UV-A + 90% RH. Contrary to the biodegradation under the humidity conditions, the mass loss of lignin was the main reason for the straw degradation of UV-A + 90% RH. It further showed that photodegradation played a central role under the high-UV irradiation and high-humidity conditions.
4. The small increase in functional diversity of straw-degrading microbial communities at the beginning and end of the experiment provided strong evidence that biodegradation played an important role in straw degradation. The straw degradation was accelerated by the combined action of photodegradation and biodegradation under the high-UV-A irradiation and high-humidity environment.

ACKNOWLEDGMENTS

The authors are thankful for the financial support from the Jiangsu Agriculture Science and Technology Innovation Fund (CX (12) 1002-3).

REFERENCES CITED

- Austin, A. T., and Vivanco, L. (2006). "Plant litter decomposition in a semi-arid ecosystem controlled by photodegradation," *Nature* 442(7102), 555-558. DOI: 10.1038/nature05038
- Austin, A. T., and Ballaré, C. L. (2010). "Dual role of lignin in plant litter decomposition in terrestrial ecosystems," *Proceedings of the National Academy of Sciences* 107(10), 4618-4622. DOI: 10.1073/pnas.0909396107
- Bailey, W. J. (1985). "Free radical ring - opening polymerization," *Die Makromolekulare Chemie* 13(S19851), 171-190. DOI: 0.1002/macp.1985.020131985113
- Baker, N. R., and Allison, S. D. (2015). "Ultraviolet photodegradation facilitates microbial litter decomposition in a Mediterranean climate," *Ecology* 96(7), 1994-2003. DOI: 10.1890/14-1482.1

- Brandt, L. A., King, J. Y., and Milchunas, D. G. (2007). "Effects of ultraviolet radiation on litter decomposition depend on precipitation and litter chemistry in a shortgrass steppe ecosystem," *Global Change Biology* 13(10), 2193-2205. DOI: 10.1111/j.1365-2486.2007.01428.x
- Brandt, L., King, J., Hobbie, S., Milchunas, D., and Sinsabaugh, R. (2010). "The role of photodegradation in surface litter decomposition across a grassland ecosystem precipitation gradient," *Ecosystems* 13(5), 765-781. DOI: 10.1007/s10021-010-9353-2
- Brink, J. V. D., Maitan-Alfenas, G. P., Zou, G., Wang, C., Zhou, Z., Guimarães, V. M., and Vries, R. P. D. (2014). "Synergistic effect of *Aspergillus niger* and *Trichoderma reesei* enzyme sets on the saccharification of wheat straw and sugarcane bagasse," *Biotechnology Journal* 9(10), 1329-1338. DOI: 10.1002/biot.201400317
- Buraimoh, O. M., Ilori, M. O., Amund, O. O., Michel, F. C., and Grewal, S. K. (2015). "Assessment of bacterial degradation of lignocellulosic residues (sawdust) in a tropical estuarine microcosm using improvised floating raft equipment," *International Biodeterioration and Biodegradation* 104, 186-193. DOI: 10.1016/j.ibiod.2015.06.010
- Choi, K.-H., and Dobbs, F. C. (1999). "Comparison of two kinds of Biolog microplates (GN and ECO) in their ability to distinguish among aquatic microbial communities," *Journal of Microbiological Methods* 36(3), 203-213. DOI: 10.1016/S0167-7012(99)00034-2
- Day, T. A., Zhang, E. T., and Ruhland, C. T. (2007). "Exposure to solar UV-B radiation accelerates mass and lignin loss of *Larrea tridentata* litter in the Sonoran Desert," *Plant Ecology* 193(2), 185-194. DOI: 10.1007/s11258-006-9257-6
- Fang, C., Radosevich, M., and Fuhrmann, J. J. (2001). "Characterization of rhizosphere microbial community structure in five similar grass species using FAME and BIOLOG analyses," *Soil Biology and Biochemistry* 33(4), 679-682. DOI: 10.1016/S0038-0717(00)00215-7
- Fierer, N., and Jackson, R. B. (2006). "The diversity and biogeography of soil bacterial communities," *Proceedings of the National Academy of Sciences of the United States of America* 103(3), 626-631. DOI: 10.1073/pnas.0507535103
- Fujii, K., Kobayashi, M., Haque, M. Z., and Takahashi, E. (2014). "Effect of aerobic periods on the production of organic acids in the incubation of rice-straw under water-logged condition: Studies on the alteration of soil microflora and their metabolism (part 1)," *Cognitive Processing* 15(3), 397-403. (in Japanese)
- Gallo, M., Sinsabaugh, R., and Cabaniss, S. (2006). "The role of ultraviolet radiation in litter decomposition in arid ecosystems," *Applied Soil Ecology* 34(1), 82-91. DOI: 10.1016/j.apsoil.2005.12.006
- Gallo, M. E., Porrás-Alfaro, A., Odenbach, K. J., and Sinsabaugh, R. L. (2009). "Photoacceleration of plant litter decomposition in an arid environment," *Soil Biology and Biochemistry* 41(7), 1433-1441. DOI: 10.1016/j.soilbio.2009.03.025
- Garland, J. L., and Mills, A. L. (1991). "Classification and characterization of heterotrophic microbial communities on the basis of patterns of community-level sole-carbon-source utilization," *Applied and Environmental Microbiology* 57(8), 2351-2359. DOI: 0099-2240/91/082351-09\$02.00/0
- Gould, J. M. (1982). "Characterization of lignin in situ by photoacoustic spectroscopy," *Plant Physiology* 70(5), 1521-1525. DOI: 10.1104/pp.70.5.1521
- Grote, E. E., Belnap, J., Housman, D. C., and Sparks, J. P. (2010). "Carbon exchange in biological soil crust communities under differential temperatures and soil water

- contents: Implications for global change," *Global Change Biology* 16(10), 2763-2774. DOI: 10.1111/j.1365-2486.2010.02201.x
- Hackett, C. A., and Griffiths, B. S. (1997). "Statistical analysis of the time-course of Biolog substrate utilization," *Journal of Microbiological Methods* 30(1), 63-69. DOI: 10.1016/S0167-7012(97)00045-6
- Henry, H. A., Brizgys, K., and Field, C. B. (2008). "Litter decomposition in a California annual grassland: Interactions between photodegradation and litter layer thickness," *Ecosystems* 11(4), 545-554. DOI: 10.1007/s10021-008-9141-4
- Huang, X., Kocaefer, D., Kocaefer, Y., Boluk, Y., and Pichette, A. (2012). "Study of the degradation behavior of heat-treated jack pine (*Pinus banksiana*) under artificial sunlight irradiation," *Polymer Degradation and Stability* 97(7), 1197-1214. DOI: 10.1016/j.polymdegradstab.2012.03.022
- King, J. Y., Brandt, L. A., and Adair, E. C. (2012). "Shedding light on plant litter decomposition: Advances, implications and new directions in understanding the role of photodegradation," *Biogeochemistry* 111(1-3), 57-81. DOI: 10.1007/s10533-012-9737-9
- Kirschbaum, M. U., Lambie, S. M., and Zhou, H. (2011). "No UV enhancement of litter decomposition observed on dry samples under controlled laboratory conditions," *Soil Biology and Biochemistry* 43(6), 1300-1307. DOI: 10.1016/j.soilbio.2011.03.001
- Kolar, J. (1997). "Mechanism of autoxidative degradation of cellulose," *Restaurator* 18(4), 163-176. DOI: 10.1515/rest.1997.18.4.163
- Lanzalunga, O., and Bietti, M. (2000). "Photo-and radiation chemical induced degradation of lignin model compounds," *Journal of Photochemistry and Photobiology B: Biology* 56(2), 85-108. DOI: 10.1016/S1011-1344(00)00054-3
- Laothanachareon, T., Bunternngsook, B., Suwannarangsee, S., Eurwilaichitr, L., and Champreda, V. (2015). "Synergistic action of recombinant accessory hemicellulolytic and pectinolytic enzymes to *Trichoderma reesei* cellulase on rice straw degradation," *Bioresource Technology* 198, 682-690. DOI: 10.1016/j.biortech.2015.09.053
- Li, Y., Huang, H., Wu, G., Yan, S., Chang, Z., Bi, J., and Chen, L. (2016). "The effects of UV-A on dry rice straw decomposition under controlled laboratory conditions," *BioResources* 11(1), 2568-2582. DOI: 10.15376/biores.11.1.2568-2582
- Lin, Y., Scarlett, R. D., and King, J. Y. (2015). "Effects of UV photodegradation on subsequent microbial decomposition of *Bromus diandrus* litter," *Plant and Soil* 395(1-2), 263-271. DOI: 10.1007/s11104-015-2551-0
- Liu, S., Hu, R., Cai, G., Lin, S., Zhao, J., and Li, Y. (2014). "The role of UV-B radiation and precipitation on straw decomposition and topsoil C turnover," *Soil Biology and Biochemistry* 77, 197-202. DOI: 10.1016/j.soilbio.2014.06.009
- Liu, Y., Wu, X., Chen, J., Chen, L., Wang, K., Su, X., Zhou, H., and Xiong, X. (2015). "Insights into the effects of γ -irradiation on the microstructure, thermal stability and irradiation-derived degradation components of microcrystalline cellulose (MCC)," *RSC Advances* 5(43), 34353-34363. DOI: 10.1039/C5RA03300D
- Malešič, J., Kolar, J., Strlič, M., Kočar, D., Fromageot, D., Lemaire, J., and Haillant, O. (2005). "Photo-induced degradation of cellulose," *Polymer Degradation and Stability* 89(1), 64-69. DOI: 10.1016/j.polymdegradstab.2005.01.003
- Müller, U., Rätzsch, M., Schwanninger, M., Steiner, M., and Zöbl, H. (2003). "Yellowing and IR-changes of spruce wood as result of UV-irradiation," *Journal of Photochemistry and Photobiology B: Biology* 69(2), 97-105. DOI: 10.1016/S1011-1344(02)00412-8

- Martins, M. R., Pereira, P., Lima, N., and Cruz-Morais, J. (2013). "Degradation of metalaxyl and folpet by filamentous fungi isolated from Portuguese (Alentejo) vineyard soils," *Archives of Environmental Contamination and Toxicology* 65(1), 67-77. DOI: 10.1007/s00244-013-9877-5
- Mohanram, S., Rajan, K., Carrier, D. J., Nain, L., and Arora, A. (2015). "Insights into biological delignification of rice straw by *Trametes hirsuta* and *Myrothecium roridum* and comparison of saccharification yields with dilute acid pretreatment," *Biomass and Bioenergy* 76, 54-60. DOI: 10.1016/j.biombioe.2015.02.031
- Pandey, K., and Pitman, A. (2003). "FTIR studies of the changes in wood chemistry following decay by brown-rot and white-rot fungi," *International Biodeterioration & Biodegradation* 52(3), 151-160. DOI: 10.1016/S0964-8305(03)00052-0
- Qu, P., Huang, H. Y., Wu, G. F., Sun, E. H., and Chang, Z. Z. (2015). "Effects of hydrolysis degree of soy protein isolate on the structure and performance of hydrolyzed soy protein isolate/urea/formaldehyde copolymer resin," *Journal of Applied Polymer Science* 132(7), 41469. DOI: 10.1002/app.41469
- Rosu, D., Teaca, C.-A., Bodirlau, R., and Rosu, L. (2010). "FTIR and color change of the modified wood as a result of artificial light irradiation," *Journal of Photochemistry and Photobiology B: Biology* 99(3), 144-149. DOI: 10.1016/j.jphotobiol.2010.03.010
- Rozema, J., Tosserams, M., Nelissen, H., Van Heerwaarden, L., Broekman, R., and Flierman, N. (1997). "Stratospheric ozone reduction and ecosystem processes: Enhanced UV-B radiation affects chemical quality and decomposition of leaves of the dune grassland species *Calamagrostis epigeios*," in: *UV-B and Biosphere*, J. Rozema, W. W. C. Gieskes, S. C. Van De Geijn, C. Nolan, and H. De Boois (eds.), Springer, The Netherlands, pp. 284-294. DOI: 10.1007/978-94-011-5718-6_25
- Santos, A. L., Oliveira, V., Baptista, I., Henriques, I., Gomes, N. C. M., Almeida, A., Correia, A., and Cunha, Â. (2013). "Wavelength dependence of biological damage induced by UV radiation on bacteria," *Archives of Microbiology* 195(1), 63-74. DOI: 10.1007/s00203-012-0847-5
- Schade, G. W., Hofmann, R. M., and Crutzen, P. J. (1999). "CO emissions from degrading plant matter," *Tellus B* 51(5), 889-908. DOI: 10.3402/tellusb.v51i5.16501
- Smith, W. K., Gao, W., Steltzer, H., Wallenstein, M. D., and Tree, R. (2010). "Moisture availability influences the effect of ultraviolet-B radiation on leaf litter decomposition," *Global Change Biology* 16(1), 484-495. DOI: 10.1111/j.1365-2486.2009.01973.x
- Song, X.-z., Jiang, H., Zhang, H.-l., Peng, C.-h., and Yu, S.-q. (2011). "Elevated UV-B radiation did not affect decomposition rates of needles of two coniferous species in subtropical China," *European Journal of Soil Biology* 47(6), 343-348. DOI: 10.1016/j.ejsobi.2011.08.008
- Song, X. Z., Zhang, H. L., Chang, S. X., Jiang, H., Peng, C. H., and Shuquan, Q. Y. (2012). "Elevated UV-B radiation increased the decomposition of *Cinnamomum camphora* and *Cyclobalanopsis glauca* leaf litter in subtropical China," *Journal of Soils and Sediments* 12(3), 307-311. DOI: 10.1007/s11368-011-0451-3
- Uselman, S. M., Snyder, K. A., Blank, R. R., and Jones, T. J. (2011). "UVB exposure does not accelerate rates of litter decomposition in a semi-arid riparian ecosystem," *Soil Biology and Biochemistry* 43(6), 1254-1265. DOI: 10.1016/j.soilbio.2011.02.016
- Wihan, J. (2007). *Humidity in Straw Bale Walls and Its Effect on the Decomposition of Straw*, Unpublished MSc thesis, University of East London, London, UK.

- Yang, L., and King, J. Y. (2014). "Effects of UV Exposure and litter position on decomposition in a California grassland," *Ecosystems* 17(1), 158-168. DOI: 10.1007/s10021-013-9712-x
- Yanto, D. H. Y., and Tachibana, S. (2014). "Potential of fungal co-culturing for accelerated biodegradation of petroleum hydrocarbons in soil," *Journal of Hazardous Materials* 278, 454-463. DOI: 10.1016/j.jhazmat.2014.06.039
- Zeng, J., Singh, D., and Chen, S. (2011). "Thermal decomposition kinetics of wheat straw treated by *Phanerochaete chrysosporium*," *International Biodeterioration and Biodegradation* 65(3), 410-414. DOI: 10.1016/j.ibiod.2011.01.004
- Zepp, R., Erickson III, D., Paul, N., and Sulzberger, B. (2007). "Interactive effects of solar UV radiation and climate change on biogeochemical cycling," *Photochemical and Photobiological Sciences* 6(3), 286-300. DOI: 10.1039/B700021A

Article submitted: July 4, 2016; Peer review completed: August 28, 2016; Revised version received and accepted: September 2, 2016; Published: September 13, 2016. DOI: 10.15376/biores.11.4.9255-9272